Revista de Metalurgia
Vol. 53, Issue 2, April–June 2017, e094
ISSN-L: 0034-8570
http://dx.doi.org/10.3989/revmetalm.94

Elasto-plastic hardening models adjustment to ferritic, austenitic and austenoferritic Rebar

Beatriz Hortigón[a,✉], José M. Gallardo[b], Enrique J. Nieto-García[a], José A. López[c]

[a] Structures Research Group. Superior Polytechnic School, University of Seville, Virgen de África 7, 41011 Sevilla, España
[b] Superior Technical School of Engineering, University of Seville, Camino de los Descubrimientos s/n, 41092 Sevilla, España
[c] Superior School of Architecture, University of Seville, Reina Mercedes 2, 41012 Sevilla, España
(✉Corresponding author: bhortigon@us.es)

Submitted: 19 September 2016: Accepted: 2 March 2017: Available On-line: 12 May 2017

ABSTRACT: The elastoplastic behaviour of steel used for structural member fabrication has received attention to facilitate a mechanical-resistant design. New Zealand and South African standards have adopted various theoretical approaches to describe such behaviour in stainless steels. With respect to the building industry, describing the tensile behaviour of steel rebar used to produce reinforced concrete structures is of interest. Differences compared with the homogenous material described in the above mentioned standards and related literatures are discussed in this paper. Specifically, the presence of ribs and the TEMPCORE® technology used to produce carbon steel rebar may alter the elastoplastic model. Carbon steel rebar is shown to fit a Hollomon model giving hardening exponent values on the order of 0.17. Austenitic stainless steel rebar behaviour is better described using a modified Rasmussen model with a free fitted exponent of 6. Duplex stainless steel shows a poor fit to any previous model.

KEYWORDS: Elastoplastic behavior; Hollomon curve; Patterned bar; Ramberg-Osgood curve; Strain hardening exponent; Stress-strain curve

Citation/Citar como: Hortigón, B.; Gallardo, J.M.; Nieto-García, E.J.; López, J.A. (2017) "Elasto-plastic hardening models adjustment to ferritic, austenitic and austenoferritic Rebar". *Rev. Metal.* 53 (2):e094. http://dx.doi.org/10.3989/revmetalm.094

RESUMEN: *Ajuste de los aceros corrugados ferríticos, austeníticos y austenoferríticos a los modelos de endurecimiento elastoplástico por deformación.* Uno de los principales factores tenidos en cuenta en la fabricación de aceros estructurales es su comportamiento durante la fase elastoplástica o de endurecimiento por deformación. Normas neozelandesas y sudafricanas plantean diversas aproximaciones teóricas para describir dicho comportamiento en el caso de los aceros inoxidables. En el campo de la construcción resulta de interés la descripción del comportamiento tenso-deformacional de los aceros corrugados utilizados en las estructuras de hormigón armado. En este artículo se discuten los modelos planteados en las normas citadas anteriormente así como los existentes en la literatura tanto para los aceros corrugados inoxidables como para los aceros al carbono fabricados mediante el proceso denominado TEMPCORE® Los aceros TEMPCORE® analizados arrojan un valor del exponente de endurecimiento por deformación según el modelo de Hollomon de 0.17. Los aceros inoxidables austeníticos se ajustan mejor al modelo de Rasmussen presentando un exponente de valor 6 realizando un ajuste libre de la función correspondiente. Para los aceros inoxidables Dúplex se obtienen muy bajos ajustes para los dos modelos citados.

PALABRAS CLAVE: Barras corrugadas; Comportamiento elastoplástico; Curva tensión-deformación; Exponente de endurecimiento por deformación; Modelo de Hollomon; Modelo de Ramberg-Osgood

ORCID ID: Beatriz Hortigón (http://orcid.org/0000-0002-3362-3648); José M. Gallardo (http://orcid.org/0000-0002-7007-2259); Enrique J. Nieto-García (http://orcid.org/0000-0001-9657-9421); José A. López (http://orcid.org/0000-0002-8227-6523)

1. INTRODUCTION

When designing a building or a structure, it is increasingly important to have analytical descriptions of the elastoplastic material behaviour. Exact knowledge is needed to supply numerical methods to produce precise results or to find analytical solutions to simple load cases. Hollomon (1945) proposed one of the very first simple equations that is still used today. Ramberg and Osgood (1943); Mirambell and Real (2000); Rasmussen (2003) and many others (Abdella, 2006; Abdella, 2007; Kang and Kan, 2007; Quach *et al.*, 2008; Abdella, 2009; Abdella *et al.*, 2011; Abbassi *et al.*, 2013; Komori, 2014) developed more elaborate formulations to be applied under specific circumstances. SABS 0162-4 (1997) and AS/NZS 4673 (2001) refer to the design models that avoid buckling in stainless steel structures.

The durability and ductility of structures are also of paramount importance in modern design and can be described using the approaches mentioned above. An interesting case that has received little attention is rebar steels. Beginning in the nineties, international standards introduced weldable steels with improved ductility. EN 1992-1-1 (2004) highlights the importance of ductility and incorporates a three level classification (A, B and C) depending on ε_{max} value. Carbon rebar steels with improved ductility obtain their unique properties through a so-called TEMPCORE® thermal production treatment, developed in 1975 by the C.R.M. Liège. This is a two step process which involves up to four different microstructural transformations. Coming immediately after the final rolling box, water jets partially quench the Rebar surface. Subsequent air cooling of the rebar core, induces martensite tempering and residual austenite bainitic transformation at the surface along with ferrite-pearlite formation at the core. The final composite structure shows an optimal balance of ductility and strength.

Currently, high ductility can also be obtained using stainless steel rebar that is hot or cold rolled. Due to its patterned shape and specific production routes, stainless steel rebar structures are far from the homogeneous materials that are used to validate the previously mentioned formulations. Nevertheless, it is well known that the ductility of reinforced concrete structures is of paramount importance when designing in areas of high seismicity. The description of plastic behaviour has been accomplished using experimental formulations (Doñate Megías *et al.*, 2003). It is convenient to determine whether plastic behaviour models can be applied to rebar with improved ductility. In this paper, the results of tensile tests of four grades of rebar steel are used to fit the Hollomon formulation as well as a slightly modified Rasmussen formulation to the experimental data. The hardening exponents found are compared to those reported in the literature.

2. MATERIALS AND METHODS

Five different grades of steel were tested: three carbon grades and two stainless grades, of which one was austenitic and the other was duplex. The carbon grades were produced using the TEMPCORE® process, but one of the grades was rolled to a plain circular section, whereas the other two grades exhibited the conventional ribs of reinforcing rebar. The stainless steel ribs were produced using cold rolling as the final shaping process. All of the ribs were selected to have a 14 mm nominal diameter (Fig. 1). Table 1 shows the mean mechanical properties determined from the tests.

Ten samples prepared from each of the grades were tested. The free length between the clamping heads was fixed at approximately 110 mm. The tensile tests were conducted according to European Standards UNE-EN-ISO 6892-1 (2010) and UNE-EN-ISO 15630-1 (2011). Additionally, 20 $MPa.s^{-1}$ was selected as the test speed during the elastic period. In determining Young modulus (E), a Class 1 extensometer was clampled down on the samples.

FIGURE 1. Reinforcing bars used in this study. (Left) Carbon round, carbon rebar and stainless steel rebar; (Right) Tempcore® structure of the carbon steel.

TABLE 1. Mechanical properties measured (mean values)

Material	f_y (MPa)	f_s (MPa)	f_s / f_y	ε_{max}	$\varepsilon_{u,5}$	E (GPa)
TEMPCORE® 1 (round)	521.22±8.23	627.45±2,57	1.21±0.02	0.106±0.003	0.261±0.008	195
TEMPCORE® 2 (rebar)	522.32±9.99	647.37±1,27	1.24±0.02	0.154±0.009	0.259±0.017	200
TEMPCORE® 3 (rebar)	545.55±4.05	678.22±2.68	1.24±0.01	0.123±0,004	0.174±0.011	187
AISI 304	752.35±11.82	878.52±6.00	1.17±0.01	0.175±0.008	0.314±0.010	197
Duplex 2205	983.54±19.35	1103.45±6.88	1.12±0.02	0.032±0.021	0.171±0.027	195

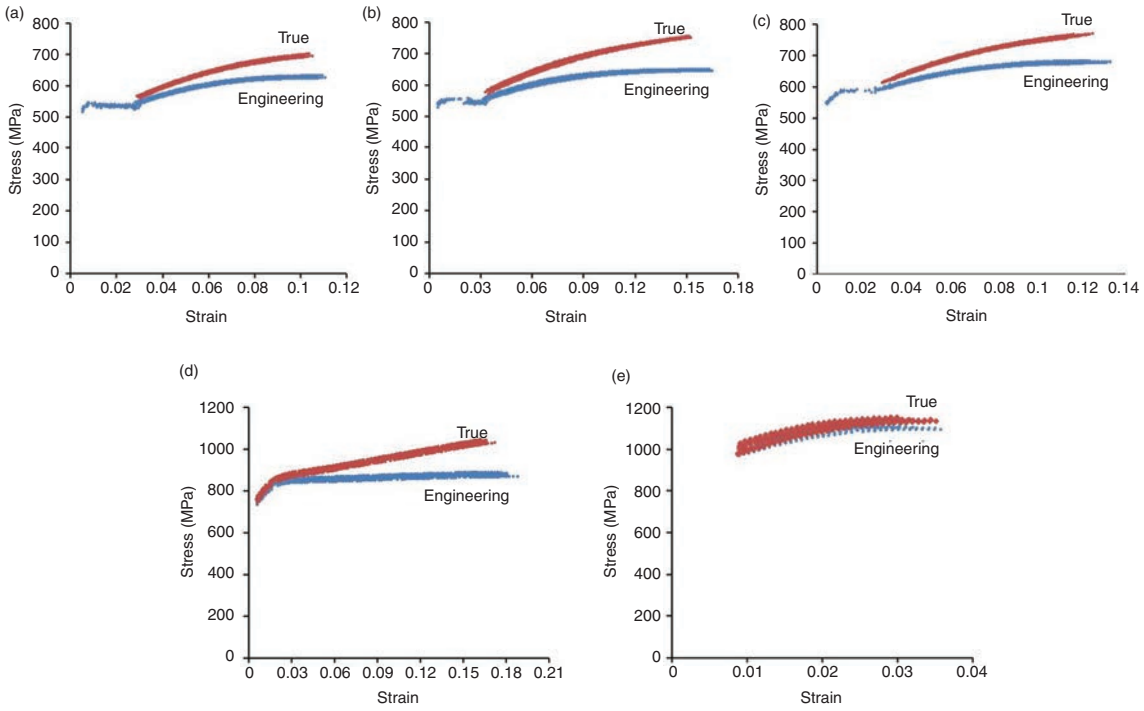

FIGURE 2. Experimental results plotted as σ vs. ε. Both the engineering and the real results are shown. From top to bottom: (a) TEMPCORE® 1 (round), (b) TEMPCORE® 2 (rebar), (c) TEMPCORE® 3 (rebar), (d) AISI 304 and (e) Duplex 2205.

Plastic behaviour data were acquired while stretching at 0.167 mm.s^{-1}. A high resolution camera and an in-house developed image analysis method (Hortigon *et al.*, 2012) was used to measure deformations at this stage.

3. RESULTS AND DISCUSSION

3.1. Results

Stress-strain data obtained by testing the five materials are represented in Fig. 2. Both the engineering and the real values are shown.

3.2. Theory and calculations

Empirical models of elastoplastic behaviour of metals are typically defined by Ramberg and Osgood (1943) and Hollomon (1945) models.

Hollomon (1945) developed the model to be applied to cold-formed steels between elastic strain at the yield stress and strain at maximum load. In this zone, the steel strain hardens according to the model $\ln \sigma_t = \ln K + n \ln \varepsilon_t$, where σ_t and ε_t are the real stress and strain according to Nadai (1950), K is a constant and n is the strain hardening exponent. Following the criteria given by Considère (1885), n can be shown to be equal to $\varepsilon_{max,t}$. Carbon steel rebar shows extensive yielding after the elastic period. It is then necessary to redefine the threshold value ($\varepsilon^p_{0,t}$, $\sigma^p_{0,t}$) for the strain hardening behaviour. A real strain value corresponding to a deformation of 0.4 mm in excess of the last minimum of the yield stress was considered. A similar protocol was described in the well-documented rebar mechanical behaviour survey by Doñate Megías *et al.* (2003). Stainless steels do not need any adjustment, and the plastic behaviour extends from a strain corresponding to the real

yield strength, $f_{y,t}$, to the real rupture strength, $f_{s,t}$ (Eq. (1)):

$$\sigma_t = K\,\varepsilon_t^{n}, \text{ which is valid for the interval } (\varepsilon^p_{0,t}, \sigma^p_{0,t}) \rightarrow (\varepsilon_{max,t}, f_{s,t}) \quad (1)$$

The elastoplastic behaviour model proposed by Ramberg and Osgood (1943) modifies the potential relationship proposed by Hollomon (1945). This model better describes materials where the transition from elastic to plastic behaviour is not easily distinguished, such as in stainless steels. The potential relationship is now applied to the plastic strain by defining the elastic portion of strain as $\varepsilon^e = \sigma/E$. Conversely, the plastic strain ε^p is a potential function of the engineering stress $\varepsilon^p = K' \sigma^{n'}$. By adding the elastic strain, it can be shown that the total strain follows $\varepsilon = \sigma/E + 0.002\,(\sigma/f_y)^{n'}$, where $n' = \ln 20/\ln(fy/\sigma_{0.0001})$. The validity of this relationship was proposed to extend up to $\sigma/\varepsilon \leq 0.9\,E$.

Mirambell and Real (2000) and Rasmussen (2003) slightly changed the Ramberg & Osgood model. Now the elastic strain is split into two regions: below (ε_y) and above the yield strength ($[\sigma - f_y]/E_{0.002}$), where $E_{0.002}$ is the tangent modulus at the yield stress and is defined as $E_{0,002} = E/(1+0.002^{*}\, n'^{*}(E/f_y))$.

Additionally, the plastic strain is referred to as the stress in excess of the yield strength ($\varepsilon^p = K''(\sigma - f_y)^m$). The value of m could be computed from a simple equation: $m = 1 + 3.5\,(f_y/f_s)$. To apply the Rasmussen model to carbon steel rebar produced by hot rolling and the TEMPCORE® process, some adjustments must be made. Again, the initial strain hardening point (ε^p_0, σ^p_0) was considered to correspond to the experimental point where the deformation was 0.4 mm in excess of the last minimum of the yield stress. Rewriting the equation results in the following (Eq. (2)):

$$\varepsilon = \varepsilon_0 + (\sigma - \sigma_0)/E_{0.002} + \varepsilon_{up}\,[(\sigma - \sigma_0)/(f_s - \sigma_0)]^m, \quad (2)$$

which is valid for the interval $(\varepsilon^p_0, \sigma^p_0) \rightarrow (\varepsilon_{max}, f_s)$, where $\varepsilon_{up} = \varepsilon_{max} - \varepsilon_0 - f_y/E_0$, and m could be computed from $m = 1 + 3.5\,\sigma_0/f_s$.

3.3. Discussion

Figure 3 includes log-log graphs showing the experimental data and the Hollomon equation best fit to the data cloud.

Table 2 lists the strain hardening exponent values. The R^2 fitting parameter when adjusting for the entire data population is also included. Computing the mean strain hardening exponent for every tensile test (Table 2) results in comparable results as the results obtained when adjusting to the entire data cloud (n values given in Fig. 3). The Hollomon model can be used to precisely describe carbon steel

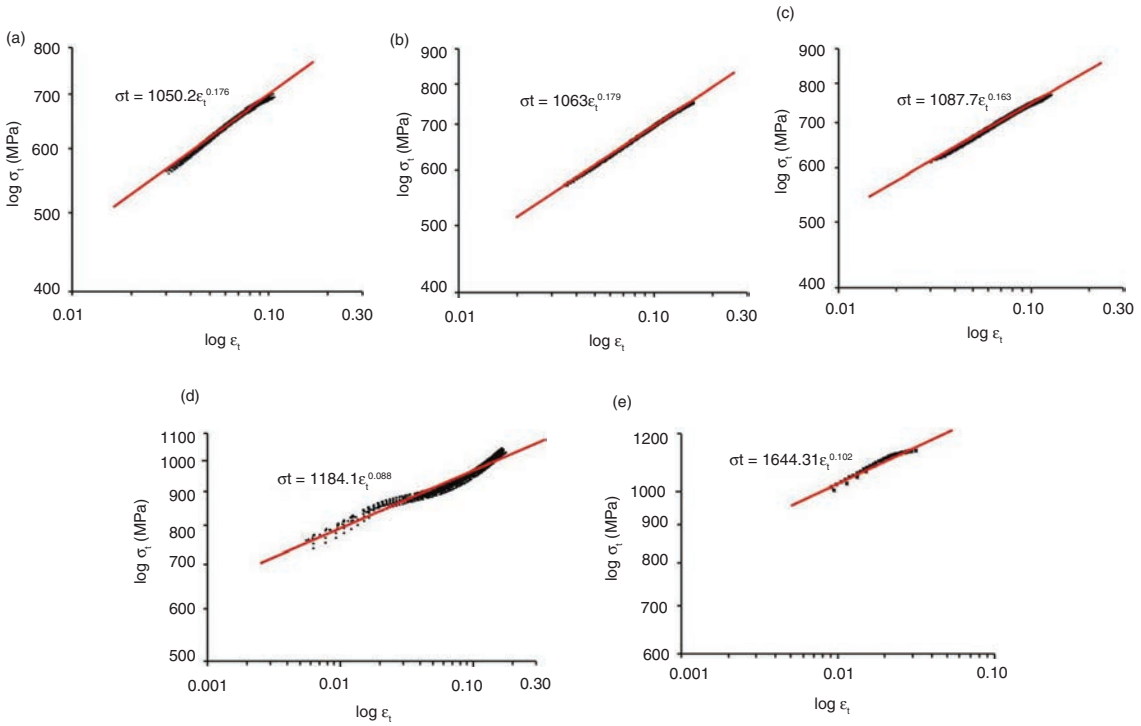

FIGURE 3. Log-log graphs and the best fit to the Hollomon equation. From the top to the bottom: (a) TEMPCORE® 1 (round), (b) TEMPCORE® 2 (rebar), (c) TEMPCORE® 3 (rebar), (d) AISI 304 and (e) Duplex 2205.

TABLE 2. Hollomon strain hardening exponent values

Material	n	R^{2*}	$\varepsilon_{max,t}$
TEMPCORE® 1 (round)	0.176±0.003	0.988	0.101±0.026
TEMPCORE® 2 (rebar)	0.179±0.003	0.995	0.143±0.074
TEMPCORE® 3 (rebar)	0.164±0.002	0.995	0.118±0.039
AISI 304	0.087±0.003	0.945	0.161±0.007
Duplex 2205	0.109±0.008	0.885	0.032±0.002

*When fitting all 10 test data samples to a single Hollomon equation. Corresponding n values shown in Fig. 3.

rebar strain hardening behaviour once the extensive yielding is complete. Statistical errors are very low, and the fitting parameter is practically in excess of 0.99. A less accurate fit is obtained when using the stainless steel data. From Fig. 3, the strain hardening log-log plot can be concluded to show an out of linear tendency for stainless steel grades.

Comparing the results of n to $\varepsilon_{max,t}$, it is evident that there is not a clear correlation even though, in all cases, $\varepsilon_{max,t}$<n except for AISI 304. The criteria given by Considerè (1885), n=$\varepsilon_{max,t}$, may be considered a condition derived from the fact that the Hollomon curve should include the coordinate ($\varepsilon_{max,t}$, $f_{s,t}$) even though this results in a poorer fit. Coming back to the experimental data curves in Fig. 3, the slope of the carbon steels and Duplex 2205 are lower as they approach $\varepsilon_{max,t}$. The observed behaviour may be attributed to ferrite phase grain refinement and deformation system exhaust as ε approaches $\varepsilon_{max,t}$. Conversely, the experimental data slope for AISI 304 increases as it approaches $\varepsilon_{max,t}$. In this case, an additional mechanism to crystal plastic deformation must be considered, namely, strain induced martensitic transformation. This, in turn, means that the criteria given by Considère may be valid in the vicinity of $\varepsilon_{max,t}$ but that the description of the entire strain hardening period is best accomplished leaving the strain hardening exponent to freely vary when computing the statistical best fit.

Comparing the n values to those found in the literature is not an easy task because, as shown by Bergström (2011), hardening behaviour described by n depends on the composition, microstructure and dislocation population. Considering only the first two conditions, Fig. 4 shows those relationships for some unalloyed steels. Greater carbon values, treatments (annealing-normalizing-hot rolling-quenching and tempering-cold rolling, in this order), which include lower tempering temperatures, appear to reduce the strain hardening capacity. The values found compare well and are slightly lower than values reported in the literature for hot rolled steels with comparable carbon content. No clear effect can be drawn as a result of the presence of ribs. In this context, it may be said that n differences among the three carbon steel rebar grades

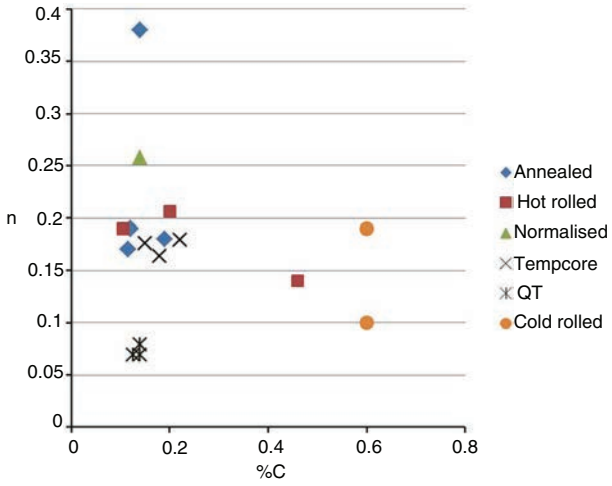

FIGURE 4. Hollomon strain hardening exponent from the literature (Dieter, 1976; Dowling, 1999; Nayebi *et al.*, 2002; Kallpakjian and Schmid, 2003; Aparicio *et al.*, 2007; Mashayekhi *et al.*, 2007).

tested are not high enough as to be easily attributed to any single small compositional or microstructural feature of the three steels.

Very scarce data on the applicability of the Hollomon model to stainless steels are available at the literature. Castro *et al.* (2001) report n values of 0.074 and 0.22 for cold and hot rolled AISI 304LN steel, respectively. Komori (2014), using a slightly modified Hollomon equation $\sigma_t = K(\varepsilon_t+0.005)^n$, found n to be 0.19 for SUS430 ferritic stainless steel. In addition to a lack of data, several factors may alter the elastoplastic behaviour, such as the deformation history or the testing speed. These data are not commonly reported in the literature.

Experimental data have also been fitted to the modified Rasmussen model. In this case, statistical regression to fit a single Rasmussen curve to the data cloud collected from all of the tests for each specimen results in a very low statistical significance. This is due to differences in the values of (ε^p_0, σ^p_0) used for each sample. With respect to the Rasmussen model, such a data pair is not only the initial data point to be fitted, as in the Hollomon model, but also modifies the parameters in the equation (2) to be fitted (see section 2: Theory and Calculations). Consequently, the individual equations have been adjusted for each sample allowing the appropriate m exponent be computed to maximise the fit. Figure 5 shows the ε-σ experimental data and the modified Rasmussen curves both using the Rasmussen-proposed m value and the value obtained from a best-fit calculation of five individual samples.

The Rasmussen model does not describe the experimental strain hardening as well as the Hollomon model does. Table 3 lists the m exponent that was computed from the Rasmussen proposal and as a free fitting value. The R^2 values are also shown.

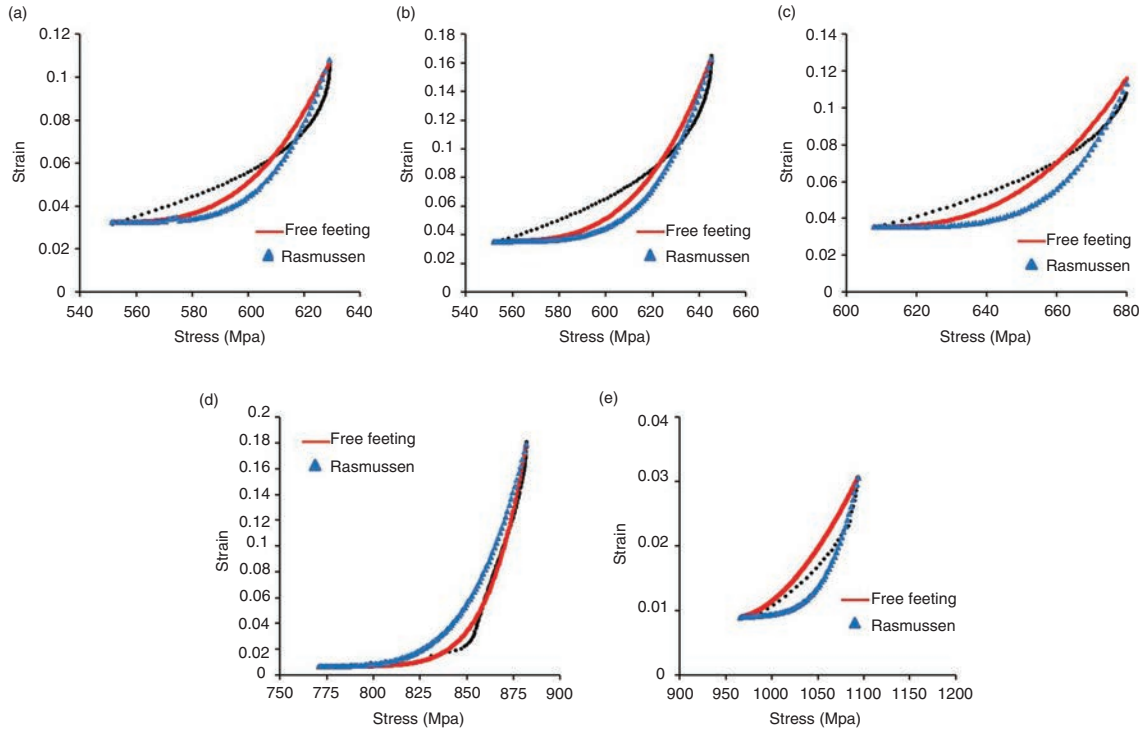

FIGURE 5. ε-σ graphs: Rasmussen model and best fit to the modified Rasmussen equation (free m value). From the top to the bottom: (a) TEMPCORE® 1 (round), (b) TEMPCORE® 2 (rebar), (c) TEMPCORE® 3 (rebar), (d) AISI 304 and (e) Duplex 2205.

TABLE 3. Rasmussen m values (according to the model and freely computed from the best fits)

Material	m_{free}	R^2	m_{Rasm}	R^2
TEMPCORE® 1 (round)	2.86±0.18	0.90±0.02	4.06±0.01	0.85±0.01
TEMPCORE® 2 (rebar)	3.14±0.47	0.91±0.04	4.04±0.02	0.86±0.06
TEMPCORE® 3 (rebar)	2.84±0.19	0.92±0.03	4.10±0.02	0.86±0.02
AISI 304	6.22±0.92	0.99±0.04	4.00±0.04	0.81±0.09
Duplex 2205	1.65±0.14	0.91±0.02	4.11±0.05	0.71±0.06

In every case, the m value computed as proposed by the Rasmussen model results in a less accurate description of the elastoplastic behaviour. Fitting is improved when the value of m is computed from the statistical methods. Generally, the values computed from the statistical methods are less than the values obtained from the Rasmussen equations. However, in the case of AISI 304 steel, where the statistically computed value was greater, a very good fit with the experimental data is obtained. This result is in agreement with the original claim from Rasmussen (2003) concerning good results when applied to stainless steels.

Comparing the values obtained in the work to the data reported in the literature is not straightforward. Mirambell and Real (2000) found m values of 3.08 and 3.68 for AISI 304 and 2205 steels, i.e., less than those computed in this paper using the formulation proposed by Rasmussen. Macdonald *et al.* (2000) reported m values of 6.22 to 7.5 when the exponent was computed by statistically fitting the free value of m. Quach *et al.* (2008) compared literature data with Ramberg and Osgood (1943) values of n', which ranged from 4.1 to 4.7 for austenitic stainless steels and from 6.2 to 7.7 for duplex stainless steels. The AS/NZS 4673 (2001) gives n' values (Ramberg and Osgood, 1943) of 7.5 for AISI 316L and 5.5 for Duplex 2205, which are both cold formed. Wang *et al.* (2014) reported some values computed with a modified equation that were slightly different from that proposed by Rasmussen and reported very low values of m of approximately 1 to 2.

4. CONCLUSIONS

- In this paper, the effect of the anisotropic structures of rebar steels along with the patterned shape on their elastoplastic hardening behaviour was investigated. Both carbon and stainless steels were tested. Experimental elastoplastic behaviour has been traditionally fitted to several well-known formulations that are typically potential relations of stress and strain. Some of these relationships have been considered by various standards to aid in structural design.
- The Hollomon model was found to precisely describe the carbon steel rebar strain hardening behaviour once extensive yielding was complete. The values found (n = 0.16-0.18) compare well to, although slightly less than, the values reported in the literature for hot rolled steels with comparable carbon content. No clear effect can be drawn resulting from the presence of ribs.
- The Rasmussen model does not describe the experimental strain hardening as well as the Hollomon model. Fitting is improved when the value of m is computed using statistical methods.
- Generally, the values computed using statistical methods are less than the values obtained using the Rasmussen equations. However, in the case of AISI 304 steel, where the statistically computed value was greater (m=6), a very good fit to the experimental data was obtained. A satisfactory fit for the behaviour of duplex rebar steel was not obtained using any of the tested models.

ACKNOWLEDGEMENTS

The authors would like to acknowledge the contribution to the experimental work carried out by J. Pinto from Superior Technical School of Engineering and R. Sánchez-Matos from the Superior Polytechnic School both at the University of Seville.

NOMENCLATURE

E: Elastic modulus
σ: Engineering normal stress
ε: Engineering strain
L_0: Gage length, which is 5 times greater than the nominal diameter
f_y: Engineering yield strength computed to a 0.002 permanent elongation
ε_y: Engineering strain at f_y
$f_{y,t}$: True yield strength
f_s: Rupture strength computed as the maximum engineering stress
ε_{max}: Engineering strain at f_s
$\varepsilon_{u,5}$: Engineering strain after break measured for the gage length
σ_t: True normal stress
ε_t: True strain
$f_{s,t}$: Rupture strength computed as the maximum true stress
$\varepsilon_{max,t}$: True strain at $f_{s,t}$ measured for the gage length
σ^p: Engineering plastic normal stress
ε^p: Engineering plastic strain
ε^e: Engineering elastic strain
$\sigma^p{}_t$: True plastic normal stress
$\varepsilon^p{}_t$: True plastic strain

REFERENCES

Abbassi, F., Mistou, S., Zghal, A. (2013). Failure analysis based on microvoid growth for sheet metal during uniaxial and biaxial tensile test. *Mater. Design* 49, 638–646. http://dx.doi.org/10.1016/j.matdes.2013.02.020.

Abdella, K. (2006). Inversion of a full range stress-strain relation for stainless steel alloys. *Int. J. Non-Lineal Mech.* 41 (3), 456–463. http://dx.doi.org/10.1016/j.ijnonlinmec.2005.10.002.

Abdella, K. (2007). An explicit stress formulation for stainless steel applicable in tension and compression. *J. Constr. Steel Res.* 63 (3), 326–331. http://dx.doi.org/10.1016/j.jcsr.2006.06.001

Abdella, K. (2009). Explicit full-range stress-strain relations for stainless steel at high temperatures. *J. Constr. Steel Res.* 65 (4), 794–800. http://dx.doi.org/10.1016/j.jcsr.2008.09.001.

Abdella, K., Thannon, R.A., Mehri, A.I., Alshaikh, F.A. (2011). Inversion of three-stage stress-strain relation for stainless steel in tension and compression. *J. Constr. Steel Res.* 67 (5), 826–832. http://dx.doi.org/10.1016/j.jcsr.2010.12.011.

Aparicio, G., D'Armas, H., Ciaccia, M. (2007). Comportamiento elastoplástico en tracción de láminas de acero ASTM A-569. *Rev. Ing.* 14 (1), 57–63.

AS/NZS 4673 (2001). *Cold-formed stainless steel structures*. Welding Technology Institute of Australia, Standards Australia International Ltd, New Zealand.

Bergström, Y. (2011). The Hollomon n-value, and the strain to necking in steel. *YB mat.* www.plastic-deformation.com/paper8.pdf.

Castro, H., Rodríguez, F.J., Belzunce, F.J. (2001). Comportamiento a fractura de aceros inoxidables austeníticos utilizados como material de refuerzo en hormigón armado. *Anales Mecánica la Fractura* 18, 124–129.

Considére, M. (1885). L´emploi du fer et de l´acier dans les constructions. *Annales Des Ponts et Chaussées* 6 (9), 574-775.

Dieter, G.E. (1976). *Mechanical Metallurgy*. 2nd Edition, McGraw Hill, Nueva York.

Doñate Megías, A., Calavera Ruiz, J., Galligo Estévez, J.M., Marí Bernat, A.R., Perepérez Ventura, B., Gómez Rey, N., Ruano Paniagua, N. (2003). *Diagramas característicos de tracción de los aceros con características especiales de ductilidad, con marca ARCER*. Monografías ARCER Nº 4. Instituto para la promoción de armaduras certificadas (IPAC), Madrid.

Dowling, N.E. (1999). *Mechanical Behaviour of Materials*. 4th Edition, Prentice Hall, Upper Saddle River.

EN 1992-1-1 (2004). Design of concrete structures. European Standard.

Hollomon, J.H. (1945). Tensile deformation. *Trans. Am. Inst. Min. Eng.* 162, 268–290.

Hortigón, B., Nieto-García, E.J., Fernández-Ancio, F., Hernández, O. (2012). Influence of corrugation shape in steel bars ductility used on reinforced concrete. *AIP Conference Proceedings* 1431, 111-117. http://dx.doi.org/10.1063/1.4707556.

Kallpakjian, S., Schmid, S.R. (2003). *Manufacturing Processes for Engineering Materials*. Prentice Hall, Upper Saddle River.

Kang, G., Kan, Q. (2007). Constitutive modeling for uniaxial time-dependent ratcheting of SS304 stainless steel. *Mech. Mater.* 39 (5), 488–499. http://dx.doi.org/10.1016/j.mechmat.2006.08.004.

Komori, K. (2014). Evaluation of ductile fracture in sheet metal forming using the ellispsoidal void model. *Mech. Mater.* 77, 67–79. http://dx.doi.org/10.1016/j.mechmat.2014.07.002.

Macdonald, M., Rhodes, J., Taylor, G.T. (2000). Mechanical properties of stainless steel lipped channels. *15th International Specialty Conference on Cold-Formed Steel Structures*, St. Louis, Missouri, USA, pp. 673-686.

Mashayekhi, M., Ziaei-Rad, S., Parvizian, J., Niklewicz, J., Hadavinia, H. (2007). Ductile crack growth based on damage criterion: Experimental and numerical studies. *Mech. Mater.* 39 (7), 623–636. http://dx.doi.org/10.1016/j.mechmat.2006.10.004.

Mirambell, E., Real, E. (2000). On the calculation of deflections in structural stainless steel beams: An experimental and numerical investigation. *J. Constr. Steel Res.* 54 (1), 109–133. http://dx.doi.org/10.1016/S0143-974X(99)00051-6.

Nadai, A. (1950). *Theory of flow and fracture of solids*. McGraw Hill, New York.

Nayebi, A., El Abdi, R., Bartier, O., Mauvoisin, G. (2002). New procedure to determine steel mechanical parameters from the spherical indentation technique. *Mech. Mater.* 34 (4), 243–254. http://dx.doi.org/10.1016/S0167-6636(02)00113-8.

Quach, W.M., Teng, J.G., Chung, K.F. (2008). Three-stage full-range stress-strain model for stainless steels. *J. Struct. Eng.* 134 (9), 1518–1527. http://dx.doi.org/10.1061/(ASCE)0733-9445(2008)134:9(1518).

Ramberg, W., Osgood, W.R. (1943). *Description of stress-strain curves by three parameters*. Report: Technical Note 902, National Advisory Committee for Aeronautics, Washington, USA.

Rasmussen, K. (2003). Full-range stress-strain curves for stainless steel alloys. *J. Constr. Steel Res.* 59 (1), 47–61. http://dx.doi.org/10.1016/S0143-974X(02)00018-4.

SABS 0162-4 (1997). *Structural use of steel. Part 4: The design of cold-formed stainless steel structural members*. The South African Bureau of Standards, Johannesburgo.

UNE-EN-ISO 6892-1 (2010). Materiales metálicos. Ensayo de tracción. Parte 1: Método de ensayo a temperatura ambiente. AENOR, Madrid.

UNE-EN-ISO 15630-1 (2011). Aceros para el armado y el pretensado de hormigón. Métodos de ensayo. Parte 1: Barras, alambres y alambrón para hormigón armado. AENOR, Madrid.

Wang, K., Carsley, J.E., He, B., Li, J., Zhang, L. (2014). Measuring forming limit strains with digital image correlation analysis. *J. Mater. Process. Tech.* 214 (5), 1120–1130. http://dx.doi.org/10.1016/j.jmatprotec.2014.01.001.